We are IntechOpen, the world's leading publisher of Open Access books
Built by scientists, for scientists

6,900
Open access books available

185,000
International authors and editors

200M
Downloads

154
Countries delivered to

Our authors are among the

TOP 1%
most cited scientists

12.2%
Contributors from top 500 universities

WEB OF SCIENCE™

Selection of our books indexed in the Book Citation Index
in Web of Science™ Core Collection (BKCI)

Interested in publishing with us?
Contact book.department@intechopen.com

Numbers displayed above are based on latest data collected.
For more information visit www.intechopen.com

4

Overtopping and Run-Up Hazards Induced by Solitary Waves and Bores

Tom. E. Baldock and Damitha Peiris
School of Civil Engineering, University of Queensland
Australia

1. Introduction

Solitary waves are wave forms that consist of a single wave, rather than waves that form part of a series of regular waves or random waves, the latter being typical of ocean wind and swell waves. A solitary wave that propagates with constant form has a unique shape for a given water depth and height, but in general, single waves of arbitrary shape are referred to as solitary waves. Single waves that have broken can be regarded as solitary bores. While the exact solitary wave shape has long been used to represent tsunami, Madsen et al. (2008) show that this is not likely to be usually the case and more complex wave shapes result. However, tsunami waves often closely resemble a solitary wave type and such waves still form the basis of most tsunami modelling. Tsunami are generated by impulsive geophysical events on ocean bed, and take the form of long waves with small steepness in the open ocean (Synolakis and Bernard, 2006). As witnessed in the 2004 Indian Ocean Tsunami, at the shore, the leading waves of a tsunami may steepen sufficiently to break and form very long surf bores.

The impact of tsunami bores may be very different to that from non-breaking or standing solitary waves, and this may require different disaster management strategies and evacuation plans, particularly when considering the initial impact and first few minutes after the wave arrival. Hall and Watts (1953) provided the first study of such waves with later laboratory studies of bore run-up providing further details on the speed of the run-up in comparison to theory (Yeh, 1991). In addition to tsunami, inundation of coastal zones by overwash is a major flooding hazard in many regions. In this instance, the overwash may be a result of run-up and overtopping on the sub-aerial beach, or as a result of overwash from waves in shallow water as the tide level inundates a barrier. In these cases, the overwash may be driven by surf zone bores or long wave surges that arise from wave groups in the shallow water or surf zone. The leading part of the long wave surge typically exhibits a solitary wave shape, as shown by Baldock (2006) and Nielsen and Baldock (2010). This overland flow in the run-up zone on beaches is frequently termed swash, and comprises an uprush (landward) and backwash (seaward) phase.

This work considers these issues, and presents the results of recent laboratory experiments measuring the overtopping flows from solitary waves and long bores. The results are discussed in the context of recent run-up theory, and used to further verify that theory for application to long bores, solitary waves and potentially initial tsunami impact. In addition, using the recent solutions, some estimates of the fluid forces, maximum inundation depths

and the potential human safety hazard arising during the run-up are presented. This chapter is organised as follows: section 2 provides an overview of previous work on tsunami, overwash, and overtopping of wave-run-up, together with an outline of the model for bore run-up (Shen and Meyer, 1963; Peregrine and Williams, 2001; Guard and Baldock, 2007). Section 3 describes the experimental setup, data collection and wave conditions in the experiments. Results and comparisons with the Guard and Baldock (2007) model are presented in section 4. Application of the model to derive flow forces and a hazard assessment in the run-up zone are discussed in section 5, with final conclusions in section 6.

2. Background

2.1 Previous studies

An extensive summary of the literature on tsunami propagation and impact is given by Synolakis and Bernard (2006). Here, the focus is on the run-up and overtopping flow, which has not been as extensively studied. Traditional tsunami models assume non-breaking waves impacting at the shoreline. In addition to the single positive "hump" of a classical solitary wave, typical tsunami also exhibit N-shaped wave forms, with either a leading depression (LDN wave) or a leading elevation (LEN wave) and the latter are primarily considered here. Additionally, tsunami waves, or the leading positive waves in a tsunami wave train, may make landfall in the form of broken waves or bores, which impact coastal defenses, beaches and lead to the initial overwash or overtopping of coastal dunes and seawalls. Eventually, the large mass of water in the main following tsunami wave overtakes the initial bore-driven run-up, generally leading to further inundation. However, initially, for the first few minutes, the impact of the tsunami may be dominated by the run-up from broken waves or bores. This initial period is important in the context of human safety on the immediate foreshore and in terms of warning systems and evacuation strategies. It is also relevant to the potential impact forces on structures, particularly if the run-up picks up debris along the coastline (Yeh, 2006). Furthermore, in the event that warnings are non-existent or too late for inland evacuation, the initial impact and human hazard are important in designing vertical evacuation strategies.

Early tsunami observations were frequently interpreted as turbulent bores (Synolakis and Bernard, 2006). Peregrine (1966; 1967) formulated the depth-averaged or non-linear shallow water (NLSW) equations that describe both the propagation and run-up of such bores. Further work by Hibberd and Peregrine (1979) provided numerical solutions for the overland or swash flows for long bores. This complemented the earlier theoretical work of Shen and Meyer (1963), later adapted by Peregrine and Williams (2001) as an analytical solution for the hydrodynamics in the swash zone. Synolakis (1987) provided solutions for the run-up of non-breaking solitary waves. However, as noted by Synolakis and Bernard (2006), run-up is still neglected in many tsunami models, which can lead to estimates of run-up that differ by factors of 2. In addition, if the run-up is not properly included in the modeling, accurate estimates of flow depths and flow velocities cannot be produced. The local bathymetry and most landward beach slope experienced by the wave is a controlling factor in the run-up and inundation (Synolakis and Bernard, 2006) and hence the wave amplitude at the original shoreline (dry beach) is important in determining the final run-up behaviour. However, most historical observations are of the maximum run-up or maximum landward penetration of tsunami waves, although post-tsunami survey data from more recent events does include inundation depths.

The solutions of the NLSW equations are applicable to describe the run-up of long bores, from which overtopping flow volumes can be determined, together with the hydrodynamics in the inundation zone. For non-breaking waves, the analytical solitary wave solutions are relevant (e.g. Carrier et al., 2003), but to the authors' knowledge have not been applied to describe overwash or overtopping volumes. Previous work has considered the classical analytical solution of Shen and Meyer (1963) to describe bore run-up and overtopping due to run-up, or swash overtopping (Peregrine and Williams, 2001). However, recent new solutions to the NLSW (Guard and Baldock, 2007) show that the Shen and Meyer solution is not conservative for engineering design, and that it significantly underestimates flow depths and overtopping flow volumes. Given that the usual criteria for human safety during flood events is based on a product of water depth and flow velocity, and that the forces on structures are proportional to the momentum flux, a product of the velocity squared and depth, the underestimation of flow depths by the traditional model can lead to significant underestimation of potential hazards.

Numerical modelling of wave overwash over steep coastal structures has used a wide range of techniques, from non-linear shallow water wave models (e.g. Kobayashi and Wurjanto, 1989; Dodd, 1998) to Boussinesq models (e.g. Stansby, 2003) to Navier-Stokes solvers (e.g. Ingram et al., 2009). A number of empirical formula are also available (Goda, 2009), although these are more applicable for sequences of periodic or random waves. However, these lose the transparency of the swash models that are controlled by the nearshore boundary conditions. On natural beaches, sand dunes and beach berms provide the first line of coastal defence, and overtopping leads to flooding of the backshore as well as the transport and deposition of marine sand and saline water. For extreme conditions, when storm surge elevations exceed the berm crest, wave overtopping may combine with a steady flood flow (Hughes and Nadal, 2009), and berm rollover and breaching of the barrier may occur. Overviews of these processes are given by Kraus et al. (2002) and Donnelly et al. (2006). Similar processes may occur due to tsunami overtopping and drawdown.

Guard and Baldock (2007) and Guard et al. (2005) proposed a new model for the run-up of long bores and leading tsunami bores. The models are written in non-dimensional form, which enables them to be applied easily to different beach slopes and run-up conditions. This model provides different solutions for different boundary conditions at the original still water line, with Shen and Meyer (1963) as a special case. The model boundary condition represents different fluxes of mass and momentum into the run-up zone, which in turn control the flow depths and magnitude of the overtopping flows if the run-up exceeds the beach length. Similar controls on the mass and momentum flux into the run-up zone could be expected for solitary-type non-breaking waves.

In natural conditions, the run-up experiences a truncated beach if the run-up exceeds the beach crest, dune crest or structure crest, and then inundation by overtopping occurs. While some previous laboratory experiments have investigated the influence of the boundary conditions on the flow depth, no previous data on overtopping of either non-breaking solitary waves or breaking solitary bores is available. Further, the theory of Guard and Baldock (2007) has not been applied to overtopping conditions, nor to estimate impact forces and hazards. This work presents some recent experiments on this issue and compares the observations with the model results. Subsequently, the model is used to illustrate how the varying boundary conditions will influence the hazards in the run-up zone in terms of flow depths and flow forces. The data and model are presented in non-dimensional form to make the results applicable over a wide range of scales.

2.2 Guard and Baldock (2007) swash model

The Shen and Meyer (1963) model is one of a number of possible solution to the nonlinear shallow-water equations (Peregrine and Williams, 2001; Pritchard and Hogg, 2005), and represents an asymptotic description of the flow close to the wave tip for a single and specific boundary condition. The solution corresponds to conditions for a dam-break wave up a slope, where the water behind the dam is initially stationary. If applied to the swash zone, this solution neglects the mass and momentum of the flow behind the incident bore front, which in many cases is very significant. Recognising this, Guard and Baldock (2007) developed new numerical solutions to the non-linear shallow-water equations that include the initial mass and momentum behind the incident bore front. An analytical form of these solutions was later developed by Pritchard *et al.* (2008), and which verified the previous numerical scheme. A brief description of the model follows, focusing on the influence of the model boundary condition on the flow depth in the run-up zone and the duration of the inflow across the original shoreline.

The model solves a non-dimensional form of NLSWE written in characteristic form as (Peregrine and Williams, 2001):

$$\frac{\partial h}{\partial t} + \frac{\partial (uh)}{\partial x} = 0$$
$$\frac{\partial u}{\partial t} + u\frac{\partial u}{\partial x} + \frac{\partial h}{\partial x} + 1 = 0 \tag{1}$$

where u and h are flow velocity and depth, respectively. The dimensionless variables are scaled as follows:

$$x = \frac{x * \sin\gamma}{A} \quad t = t * \sin\gamma\sqrt{\frac{g}{A}} \quad h = \frac{h * \cos\gamma}{A} \quad u = \frac{u *}{\sqrt{gA}} \tag{2}$$

where dimensional variables are starred and A=R/2, where R is the maximum run-up elevation above the initial elevation. For most natural beaches, cosγ can be taken equal to one, and sinγ ≈ γ. Substituting for the non-dimensional shallow water wave speed,

$$c = \sqrt{h} \tag{3}$$

these equations may be rearranged to obtain:

$$\left(\frac{\partial}{\partial t} + (u+c)\frac{\partial}{\partial x}\right)(u+2c+t) = 0$$
$$\left(\frac{\partial}{\partial t} + (u-c)\frac{\partial}{\partial x}\right)(u-2c+t) = 0 \tag{4}$$

Using the characteristic variables $\alpha(x,t)$ and $\beta(x,t)$ gives:

$$\frac{d}{dt}\alpha = 0 \quad \text{on} \quad \frac{dx}{dt} = u + c \tag{5}$$

$$\frac{d}{dt}\beta = 0 \quad \text{on} \quad \frac{dx}{dt} = u - c \tag{6}$$

where

$$\begin{aligned} \alpha(x,t) &= u + 2c + t \\ \beta(x,t) &= u - 2c + t \end{aligned} \tag{7}$$

The solutions and model results are controlled by the value of $\alpha(t)$ on the seaward swash boundary and the Shen-Meyer solution corresponds to a constant value of $\alpha=2$, which results in very shallow inundation depths. The key change introduced by Guard and Baldock (2007) allowed the value of the characteristic variable on the seaward boundary, α, to vary over time, such that:

$$\alpha(x_b, t_b) = 2 + k t_b \tag{8}$$

where $k=0$ corresponds to the Shen-Meyer solution and k is expected to lie in the range $0 < k < 1.5$, with $k=1$ corresponding to a uniform incident bore. The solutions in non-dimensional form are independent of beach slope, γ, and run-up amplitude (2A). Consequently, the Shen and Meyer solution is identical for all run-up events (there is only a single solution for $k=0$), but the Guard-Baldock model allows different boundary conditions for different incident wave types or conditions, by specifying different values for k.

Varying the model conditions on the seaward boundary, by varying $\alpha(t)$ on the incoming characteristics, results in deeper and less asymmetric swash flows than predicted by the Shen-Meyer solution. This physical significance of the characteristic values α and β is shown by the non-dimensional volume flux, q, and momentum flux, M, per unit length of wave crest which are:

$$\begin{aligned} q &= uh = \frac{1}{32}(\alpha + \beta - 2t)(\alpha - \beta)^2 = q^* \frac{\cos\gamma}{\sqrt{gA^3}} \\ M &= u^2 h = \frac{1}{64}(\alpha + \beta - 2t)^2(\alpha - \beta)^2 = M^* \frac{\cos\gamma}{\rho g A^2} \end{aligned} \tag{9}$$

Here, the starred variables are again dimensional, and the scaling follows that of Peregrine and Williams (2001), where A is half of the vertical run-up elevation above the still water shoreline, i.e. R=2A.

The interpretation in terms of the overall fluid physics is that solutions for different $\alpha(t)$ correspond to different mass and momentum flux at the seaward boundary. By varying k, and consequently $\alpha(t)$, the incoming mass and momentum fluxes at the seaward boundary can differ for each swash event, which results in different flows within the swash zone. Increases in k represent more sustained inflow conditions and lead to solutions that have a longer duration of inflow across the original shoreline, later times of flow reversal, increased depths in the swash, and a more symmetric velocity field between uprush and backwash. Figures 1 and 2 illustrate how the flow depths, the flow volume and the time of flow reversal are influenced by the choice of k. The time of flow reversal at the seaward boundary of the swash varies significantly for solutions between $k=0$ and $k=1$; at the seaward swash boundary flow reversal occurs after one-quarter of the whole swash cycle for $k=0$, whereas

for *k*=1 flow reversal occurs approximately half-way through the swash cycle (Guard and Baldock, 2007). This leads to much greater volumes of water entering the swash zone than predicted by the Shen-Meyer solution, which was originally observed on the basis of overtopping experiments using monochromatic waves by Baldock et al. (2005). Thus, the specified boundary condition, as defined by *k*, controls the overall asymmetry of the flow field, the flow depth (figure 2) and the quantity of fluid that can be expected to overtop a truncated beach.
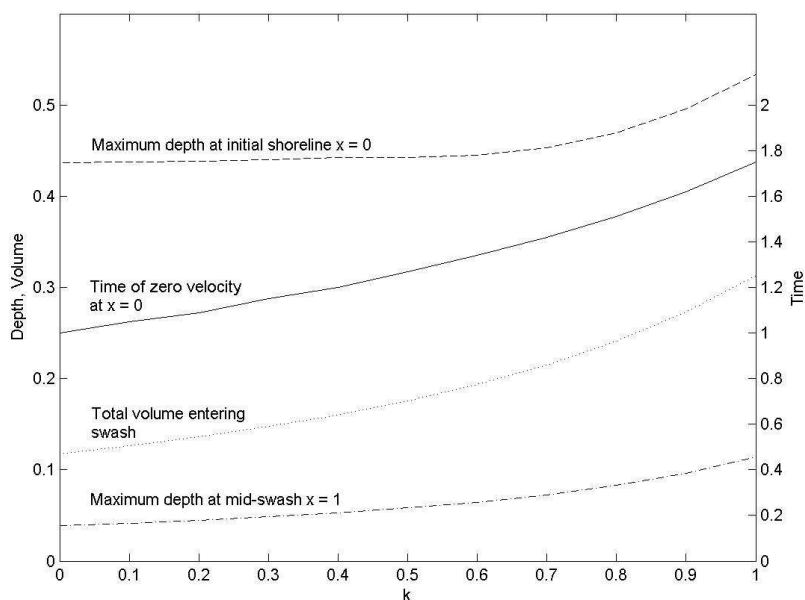
Fig. 1. The dependence of key swash hydrodynamic parameters on the swash boundary condition, parameterised through *k*. After Guard and Baldock (2007).
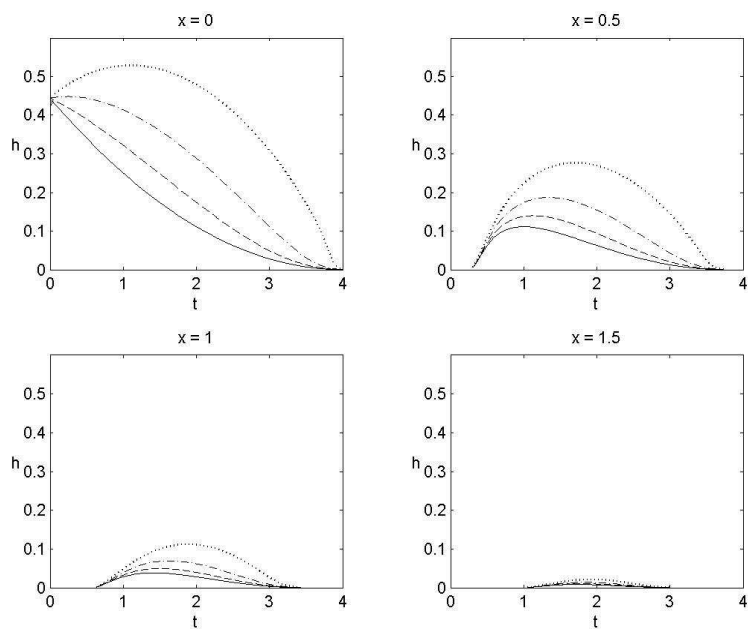
Fig. 2. Time-history of flow depth at different cross-shore locations indicated. Solid line, *k*=0 (SM63); Dashed-dotted line, *k*=1/3; Dashed line, *k*=2/3; dotted line, *k*=1. x varies from 0 at the SWL to 2 at the run-up limit. After Guard and Baldock (2007).

3. Experimental setup

3.1 Wave flume and instrumentation

The overtopping experiments were conducted in a 0.85 m wide, 0.75 m deep and 28 m long wave flume in the Gordon Mckay Hydraulics Laboratory at the University of Queensland. The bathymetry comprises of a 10.5m long horizontal section from the wavemaker to the toe of a uniform long sloping beach of gradient 0.11. The sloping beach was constructed in two parts; a fixed lower section below the water line and an adjustable beach with removable panels above the still water line. Figure 3 and figure 4 illustrates the general arrangement, where the origin of the horizontal coordinate is at the still water line (SWL) and positive onshore. Two configurations of the bed were used, firstly a smooth painted marine plywood bed, and secondly, with the bed covered by sand paper (0.2 mm grain size). The removable panels on the upper beach can be replaced by an overtopping tank sunk within the bed at
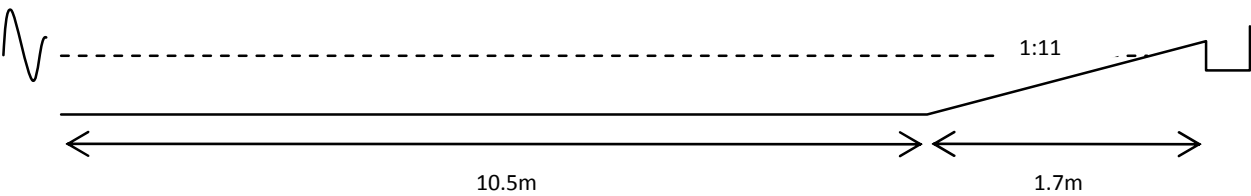
Fig. 3. Schematic of wave flume and overtopping tank for one tank position.
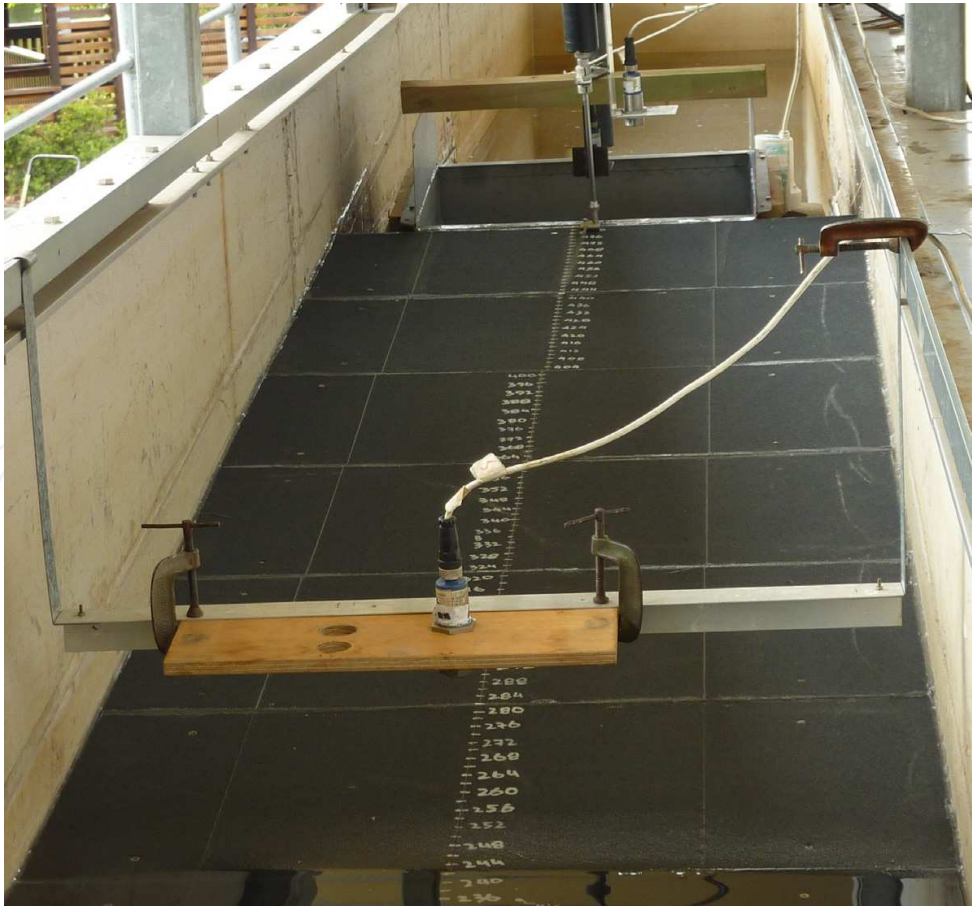

Fig. 4. Photo of upper beach panels, overtopping tank and instrumentation.

different elevations relative to the still water line and the maximum run-up. A special tank was designed, which encompassed the middle two-thirds of the flume to avoid wall effects, and which also included thin "wing" walls to prevent flow from entering from the sides (figure 4). The tank is 0.55m in length, 0.45m in width, and 0.195m deep, and results in a truncated beach at the seaward or offshore edge of the tank. The tank edge has very little effect on the uprush flow since the flow at the edge is super-critical for the majority of the uprush (Peregrine and Williams, 2001) and as shown later.

The experiments were performed with the overtopping tank located at six locations along the beach, ranging from 0.05-0.26m above the still water line. The water depth over the horizontal section of the flume was also varied, which additionally changes the tank positions relative to the SWL.

The tank position is written in non-dimensional form, such that the non-dimensional position, or truncation point for the beach, is given by E=2z/R, where R is the maximum vertical run-up excursion for each individual wave condition, and z is the elevation of the tank edge relative to the still water line (SWL). Hence, E ranges from zero, at the SWL, to two, at the run-up limit, for each particular test. This follows the Peregrine and Williams (2001) scaling. R was determined for each wave condition by running the identical experiment with a non-truncated beach without the tank, again for both the smooth and sandpaper bed surfaces. Overtopping volumes were measured in the tank using an ultrasonic distance sensor to measure the surface elevation change between the start and end of the test, with a calibrated conversion function to account for small differences in tank area with water surface elevation. The hydrodynamics were obtained from ultrasonic displacement sensors and an Acoustic Doppler Velocimeter (ADV), mounted at different locations along the flume. However, for the present work, only the ultrasonic displacement sensor data are used; the ADV and one ultrasonic sensor provide hydrodynamic boundary condition data for future numerical modelling purposes.

3.2 Wave conditions

Solitary type waves and solitary broken waves (bores) were generated using a computer-controlled hydraulic piston wave generator which has stroke lengths of up to 1.2m to generate long bores. The waves were generated by applying a known voltage signal to the wave paddle, which were generated using either error functions or using the method developed to generate solitary waves as per Goring (1979) and Baldock et al. (2009). The wave height and wavelength is controlled by varying the stroke (distance moved) and speed of the wavemaker. This has the effect of altering the hydrodynamics of each wave case, particularly the duration of the inflow into the swash zone, and therefore corresponds to waves which generate different swash boundary conditions or waves that are described by different values of *k*. The wavemaker motion and resulting wave forms are very repeatable, enabling the use of multiple tank positions and repeat runs of the same wave form. Two wave types were used in this study; waves that broke at the shore (shore breaks), and breaking waves that broke prior to reaching the SWL forming well-developed bores. This distinction was made through visual observation for each case. Altogether, 19 different wave conditions were used, repeated for four different water depths and six different (in absolute elevation) tank positions. For each wave condition, this provides measurements of the overtopping at 15-20 different truncation points between the SWL and maximum run-up.

4. Experimental results

4.1 Run-up

This section presents measurements of the run-up for the different wave conditions and surface roughness. The data are non-dimensionalised using the offshore water depth, following Hall and Watts (1953) and later researchers. Figure 5 illustrates the variation of the maximum run-up elevation, R, over the smooth bed with the maximum inundation depth or bore height measured at the SWL, H_b. Non-dimensionalising by the offshore water depth does not fully remove the depth-dependency from the data, showing that the maximum run-up is not a linear function of offshore water depths. However, the differences for water depths of 15-26cm are relatively small, and it is only for the smallest water depth that a significant difference occurs. R/d is well correlated with H_b/d, and the coefficient of proportionality ranges from 3-4, i.e. $R=CH_b$, where $3<C<4$ for these data. If the wave height at the toe of the beach is chosen for the correlation instead of H_b, the data for R/d tend to collapse more onto a single line (i.e. a linear depth dependency), but the scatter in the data is significantly greater. The relationship between run-up and offshore or nearshore wave height is therefore similar too, but not exactly the same as the theoretical and observed behaviour of non-breaking solitary waves, which show R/d is proportional to $(H/d)^{5/4}$ (Synolakis, 1987).

The behaviour is very similar on the rough slope (figure 6), and the coefficients of proportionality do not change significantly, ranging from 3-3.7. This is consistent with previous run-up measurements and suggests that the frictional effect at the wave tip is quite small. Even though the relative roughness has changed by an order of magnitude, the increased roughness reduces the run-up by only 5-10%. The non-dimensional run-up coefficients are however different from that observed by Baldock et al. (2009), which was
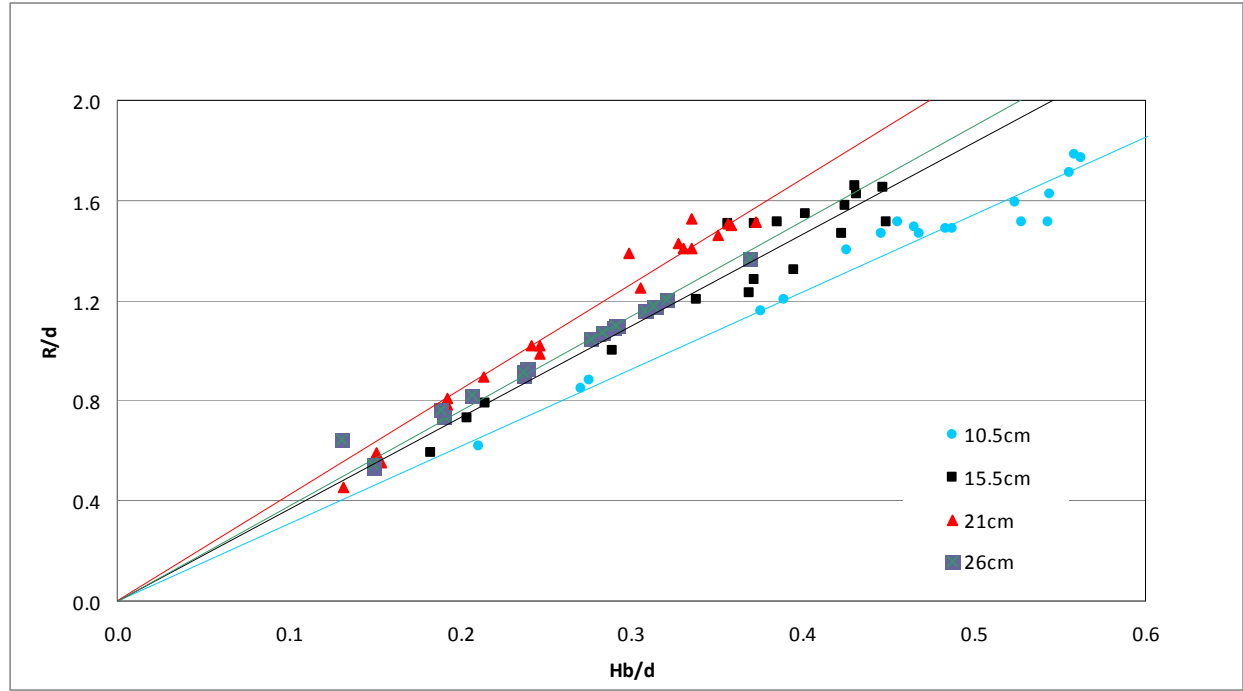

Fig. 5. Non-dimensional run-up versus maximum non-dimensional wave elevation at the still water shoreline. Smooth beach. Legend indicates water depths for each data series.
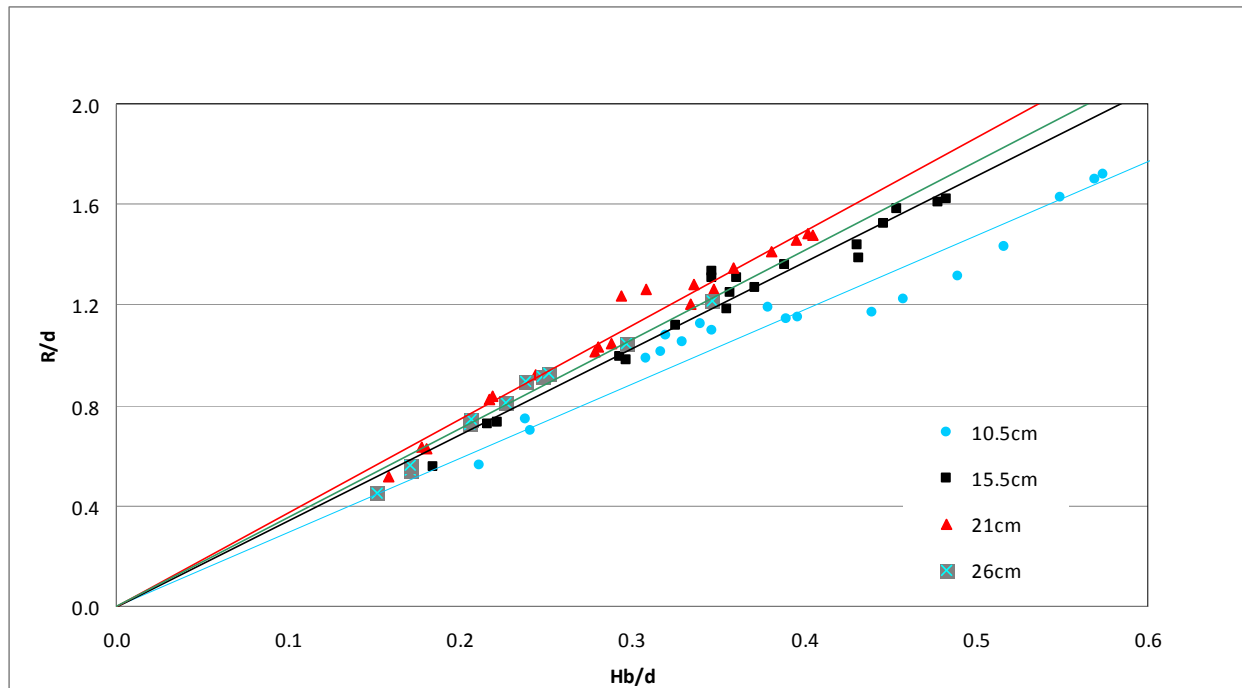
Fig. 6. Non-dimensional run-up versus maximum non-dimensional wave elevation at the still water shoreline. Rough beach. Legend indicates water depths for each data series.

C=2.6, where upper beach was a milder gradient than the offshore beach gradient. The lack of sensitivity of the run-up to the change in roughness is for two reasons; firstly, at laboratory scale Reynolds numbers, the friction factors are not expected to vary significantly with changes in relative roughness, as shown on classical diagrams, e.g. the Moody diagram; and secondly, the run-up tip does not travel as a solid body, but is constantly overrun by the flow behind (Barnes and Baldock, 2010). The latter effect further reduces the influence of friction on the thin run-up tip. Based on the Guard and Baldock (2007) model, the maximum depth at the SWL is about one-quarter of the run-up elevation (see figure 1), or alternatively, R≈4H$_b$ for k≈O(1), so the data is consistent with the theory, allowing for frictional effects. No obvious difference in run-up trend was observed between shore breaks and developed bores.

4.2 Overtopping

The type of incident wave is illustrated in figure 7, which shows the time-history of the water surface elevation at the SWL-beach intersection (original shoreline) for 3 different incident waves, W1-W3. The wavemaker stroke length and speed varies for each case, leading to a weak shore break (W1), a strong shore break (W2) and a fully developed bore (W3), respectively. The product of velocity and flow depth during the inflow to the swash zone varies for each case, which controls the overtopping rate higher on the beach face at the truncation point. This variation cannot be predicted by the Shen and Meyer (1963) solution, since all incident waves have the same boundary condition.

The measured overtopping volume per unit width of beach, V*(E), is non-dimensionalised following Peregrine and Williams (2001) as follows:
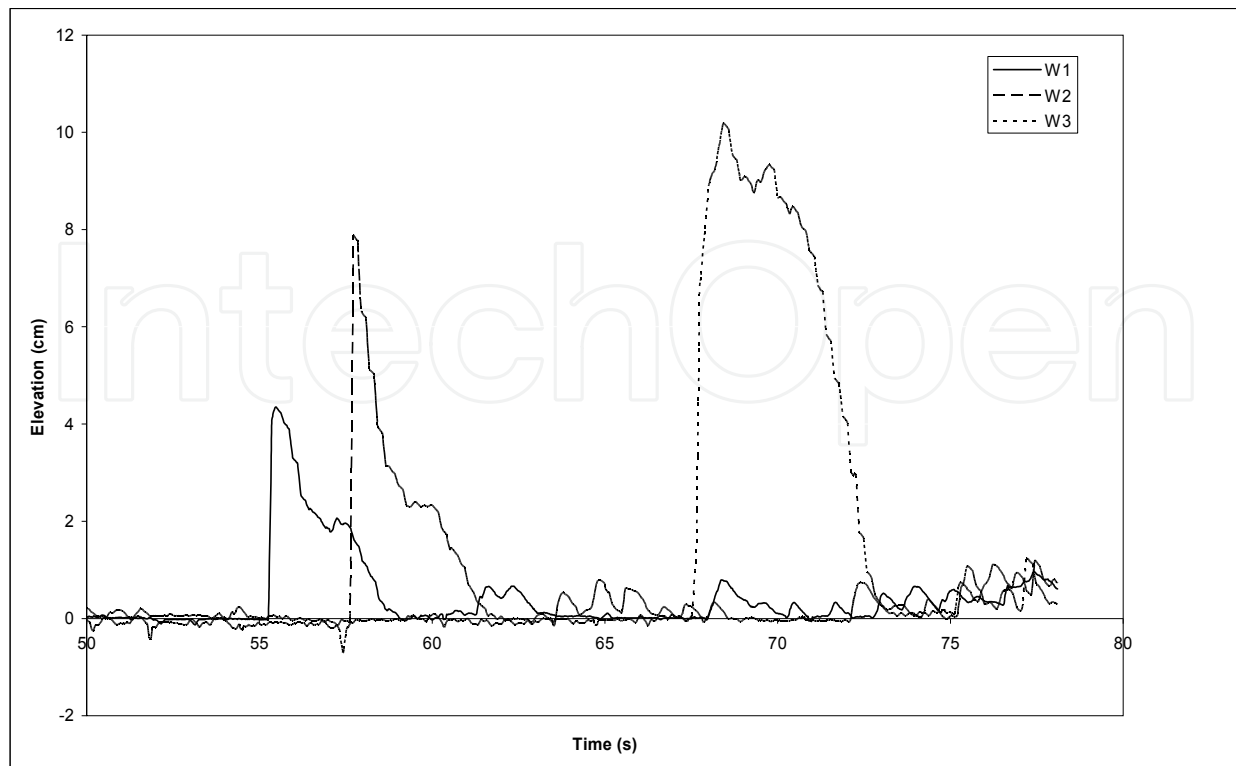
Fig. 7. Water surface elevation at the original still water shoreline for different wave types, corresponding to a weak shore break (W1), a strong shore break (W2) and a fully developed bore (W3).

$$V(E) = V^*(E)\sin(2\gamma) / 2A^2 \tag{10}$$

The non-dimensional overtopping volumes are plotted versus the relative truncation elevation , E, of the beach, where E=2z/R such that E=0 at the SWL and E=2 at the run-up limit for each wave condition. Figures 8 and 9 illustrate the data for shore break waves and fully developed bores, respectively. The theoretical overtopping derived by Peregrine and Williams (2001), itself based on the swash theory of Shen and Meyer (1963), and the empirical overtopping curve of Baldock et al. (2005) are also shown.

A distinct difference is observed between the two wave types. Waves that break at the shore generally result in smaller overtopping dimensionless volumes, and the relationship between V(E) and truncation point is quite different from that for bores. For bores, the overtopping rates increase rapidly as E decreases, whereas for the waves breaking at the shore the rate of increase is less sensitive to E. Further, the overtopping rate for the developed bores is multi-valued for the same value of E, in contrast to the shore break conditions which shows a relatively consistent trend with E, and in contrast to the Peregrine and Williams solution. This is not scatter in the data, as shown below, and is consistent with the theory of Guard and Baldock (2007). If data for a single constant offshore water depth is considered in isolation, these differences between the shore breaks and developed bores are even more marked (figure 10). The non-dimensional overtopping rate for shore breaks becomes insensitive to E, whereas for the developed bores the overtopping is not solely determined by E, and that it is again multi-valued for constant E.
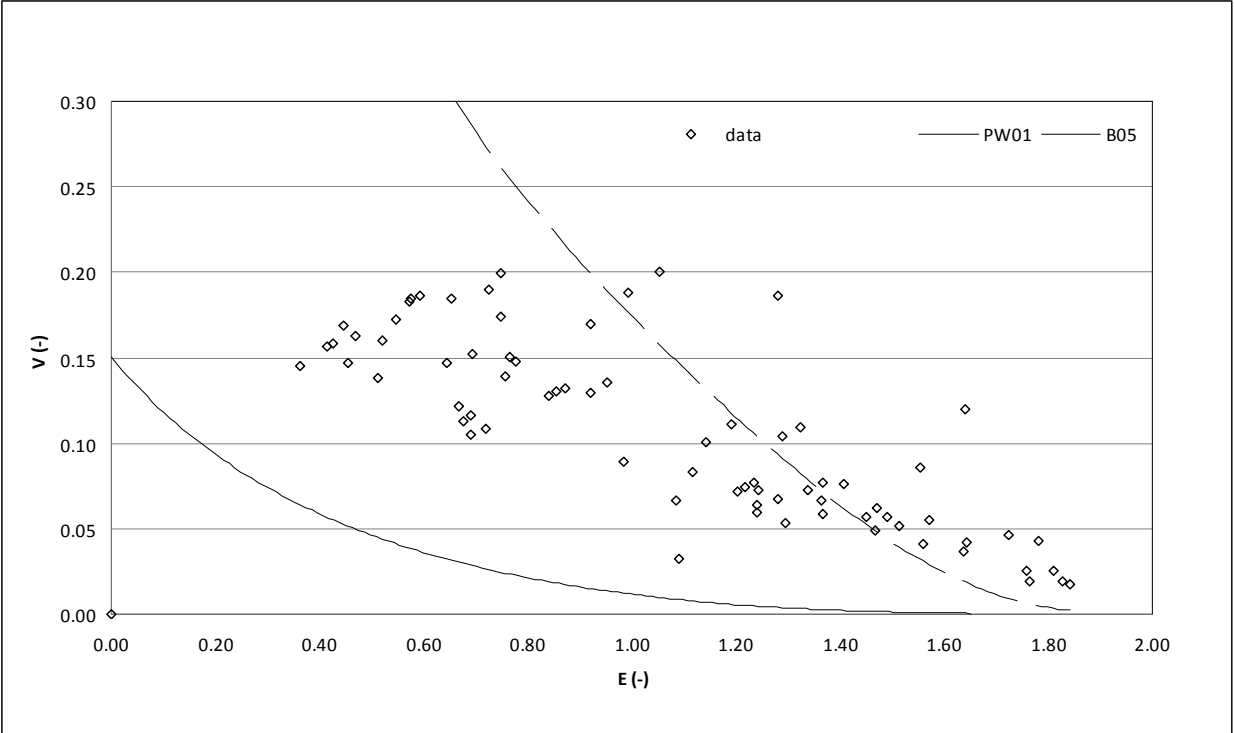
Fig. 8. Non-dimensional overtopping volume versus non-dimensional truncation point. Shore break waves and smooth beach. Legend indicates theoretical curve (solid line) of Peregrine and Williams (2001) and empirical curve (dashed line) of Baldock et al. (2005)
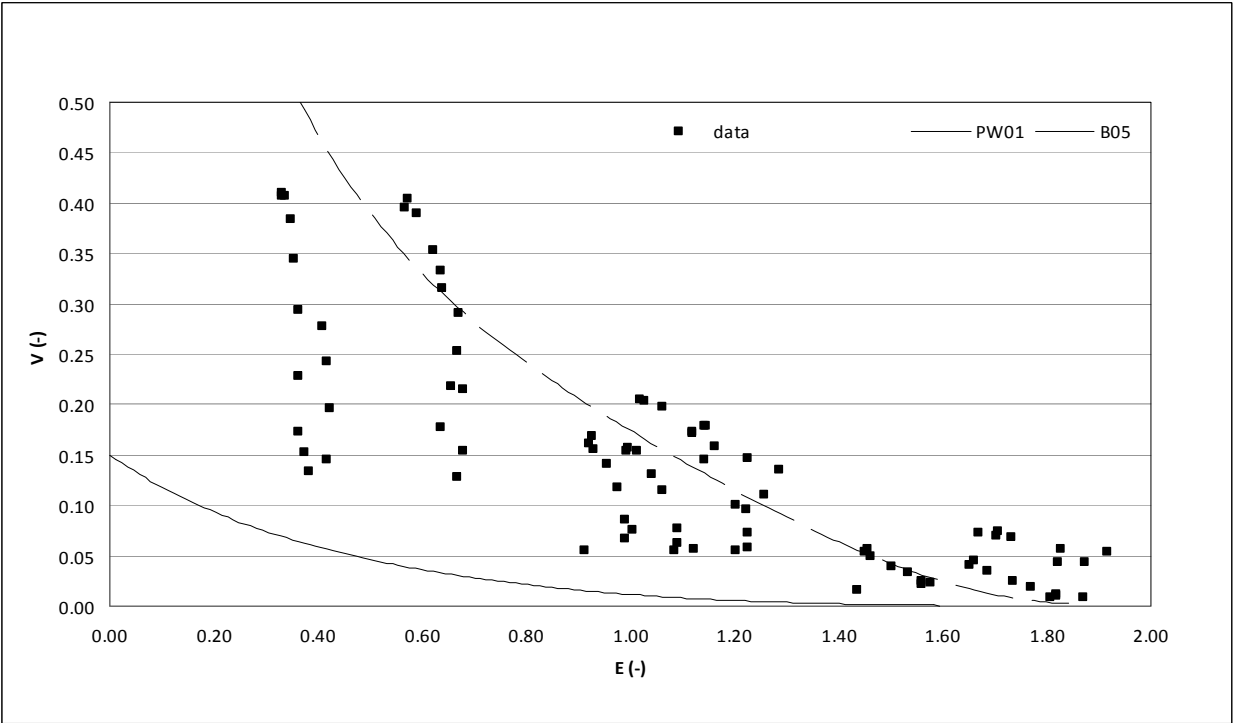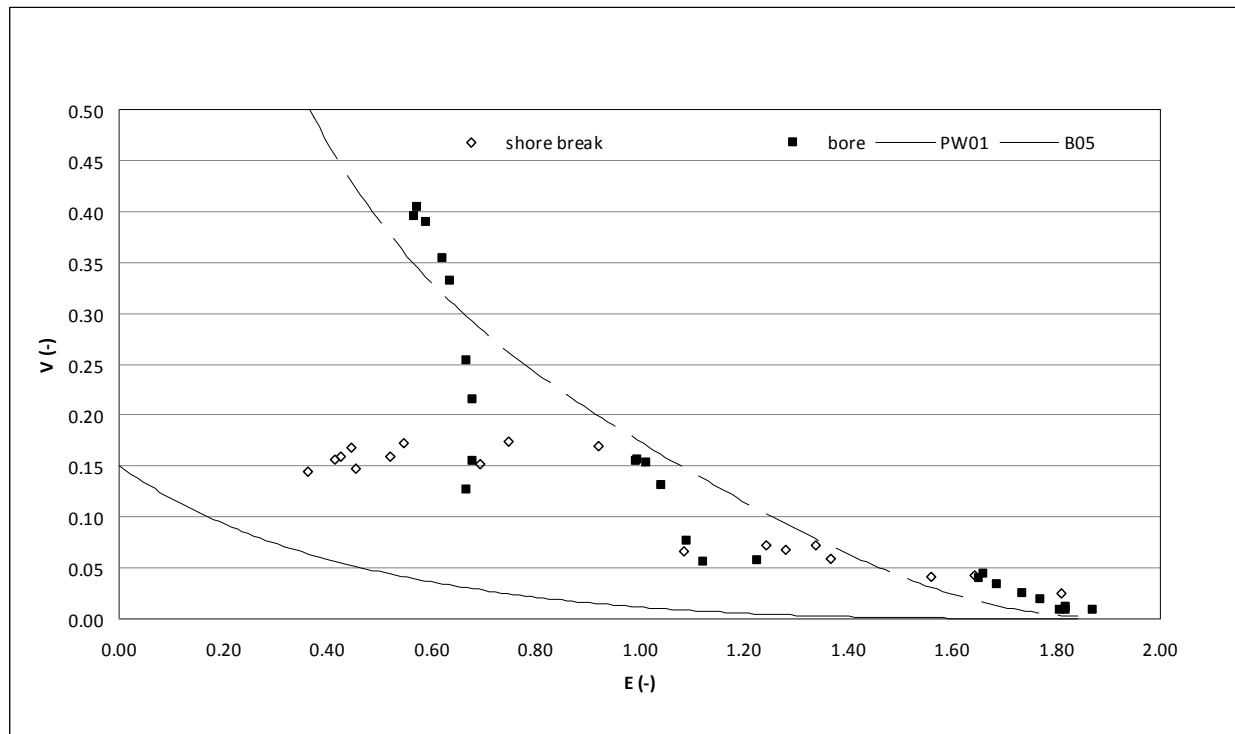

Fig. 9. Non-dimensional overtopping volume versus non-dimensional truncation point. Developed bores and smooth beach. Legend indicates theoretical curve (solid line) of Peregrine and Williams (2001) and empirical curve (dashed line) of Baldock et al. (2005)

Fig. 10. Non-dimensional overtopping volume versus non-dimensional truncation point. Shore breaks and developed bores, smooth beach, depth=15.5cm. Legend indicates theoretical curve (solid line) of Peregrine and Williams (2001) and empirical curve (dashed line) of Baldock et al. (2005).

For the developed bores, V(E) is a monotonic function of E for large E, consistent with the asymptotic solutions of the NLSWE close to the run-up limit. However, for smaller values of E, both the dimensional and the non-dimensional overtopping rates are very dependent on the incident bore conditions. Hogg et al. (2010) have further developed semi-analytical theoretical solutions to account for the variation of the overtopping rates as k is varied in the Guard and Baldock (2007) swash model. It is of interest that for E>1, the overall trend of V(E) is similar for the two different wave types. For the rough beach the trends are very similar, and as a function of E, the non-dimensional overtopping volumes do not decrease significantly (not shown).

The non-dimensional overtopping volumes obtained from the Guard and Baldock (2007) solution, and ignoring the influence of the edge on the flow, are shown in figure 11. These calculations determine the overtopping volume from the product V(E)=uh at the truncation point, but do not account for the influence of the truncation point on the flow further offshore. However, the edge does not influence the flow until the flow drops to critical conditions at the edge and Peregrine and Williams (2001) show that the supercritical overtopping volume and the total overtopping volume are similar for E>0.4 and very similar for E>1. Hence, some differences are expected between the full solution and the approximate calculations for small E. The full solution for k=0 and the approximate solution are in very good agreement for E>0.4, which shows the influence of the edge is indeed minor for most practical applications. Note that E<0.4 corresponds to locations in the lower (most seaward) fifth of the swash zone, i.e. z/R<0.2.
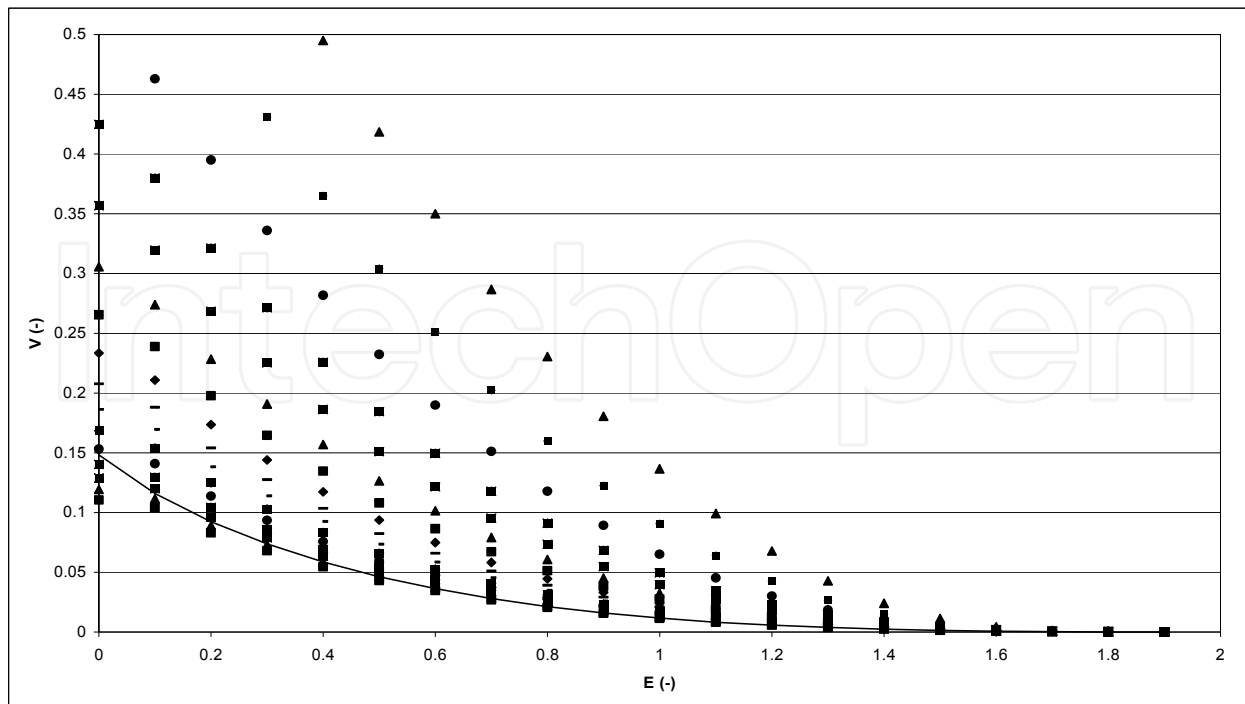
Fig. 11. Non-dimensional overtopping volume versus non-dimensional truncation point based on Guard and Baldock (2007) solution and ignoring the influence of the edge on the flow. Symbols show influence of varying *k*, from *k*=0 to *k*=1.5 at intervals of *k*=0.1. Solid line is theoretical curve of Peregrine and Williams (2001).

For *k*=0, it appears that the presence of the edge increases the volume flux past a given elevation in comparison to the solution for a non-truncated beach. This might be expected on the basis of a reduction in pressure at the free overfall and the formation of a classical M2 flow profile seaward of the edge, which reduces the gradient of the adverse (offshore dipping) water surface slope further offshore and hence reduces the influence of gravity in slowing the uprush flow.

The different symbols in figure 11 at constant values of E show the influence of varying *k*, or varying the incident mass and momentum flux in the incoming bore. The predicted overtopping volume increase by a relatively constant factor of about 2.6 as *k* increases from *k*=0 to *k*=1, and increase further to O(10) for *k*=1.5. More importantly, the predicted multiple values of V(E) at constant E are entirely consistent with the observations and in complete contrast to the monotonic solution predicted by Peregrine and Williams (2001). Comparing figure 11 with figure 9 shows that the model underestimates the measured non-dimensional overtopping volumes to some extent for E>1. However, the range of variation in the predicted and measured overtopping at a constant value of E is very similar, as illustrated in figure 12. The predicted overtopping volumes for *k*=0.9 and *k*=1.4 encompass the range of data in these experiments. This is consistent with the previous estimates of *k* for developed bores (Guard and Baldock, 2007) and from field observations of surf zone bores and swash run-up (Power et al., 2009).

It should be noted that the model is based on inviscid flow conditions. Therefore, the absolute values of the measured non-dimensional overtopping rates are sensitive to the influence of friction, which will have the greatest effect on the thin run-up tip and hence the value of R. For a real swash, the maximum run-up is expected to be reduced by a greater
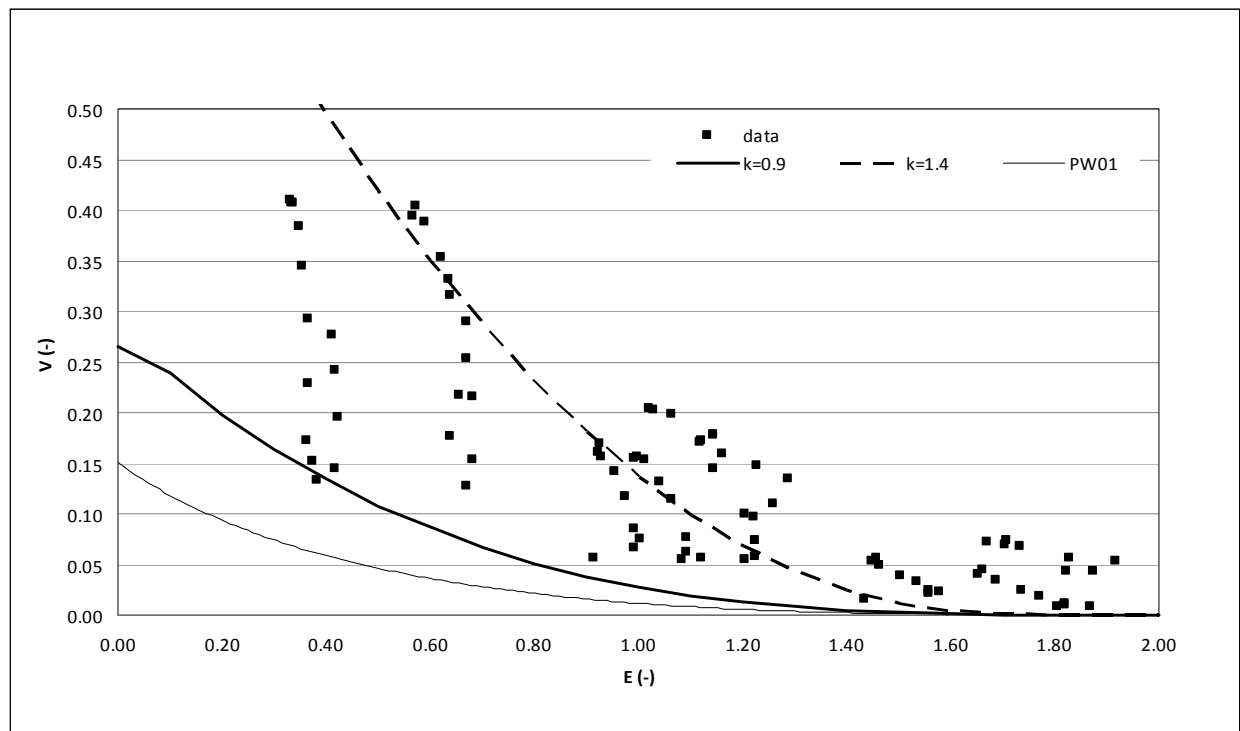
Fig. 12. Non-dimensional overtopping volume versus non-dimensional truncation point compared to range expected from Guard and Baldock (2007) solution. Developed bores and smooth beach. Thin solid line is theoretical curve of Peregrine and Williams (2001), thick solid line and thick dashed line correspond to solutions for *k*=0.9 and *k*=1.5, respectively.

extent than the depth and flow velocity at the edge, since frictional effects are greatest in the shallow flow depths at the wave tip. Thus, R is reduced in the experiments in comparison to the inviscid solution, whereas the dimensional overtopping volume is probably not reduced to such an extent. The non-dimensionalisation therefore increases the measured V(E) compared to the inviscid solution, as shown by comparing figures 9 and 11. Alternatively, this is equivalent to the value of E for the measured data being slightly too large, since they are based on the measured run-up, not the idealised inviscid run-up, which will be larger.

5. Run-up hazards

5.1 Personal safety

The ability of people to maintain a secure footing in flood flow is determined by both the flow depth and the flow velocity. For characterising flood risks to personal safety, a simple and widely used parameter is based on the product of water depth and flow velocity exceeding a critical value, typically, $u*h*>0.5-1$ (Abt et al., 1989; Ramsbottom et al., 2003). The dimensionless value of this parameter is

$$uh = \frac{u * h * \cos\gamma}{A\sqrt{gA}} \tag{11}$$

This is plotted in figures 13a&b, for uprush and backwash, respectively, and again for a range of *k* values, from which values of *u*h* can be determined for any location in the run-up zone for any particular bore run-up amplitude.
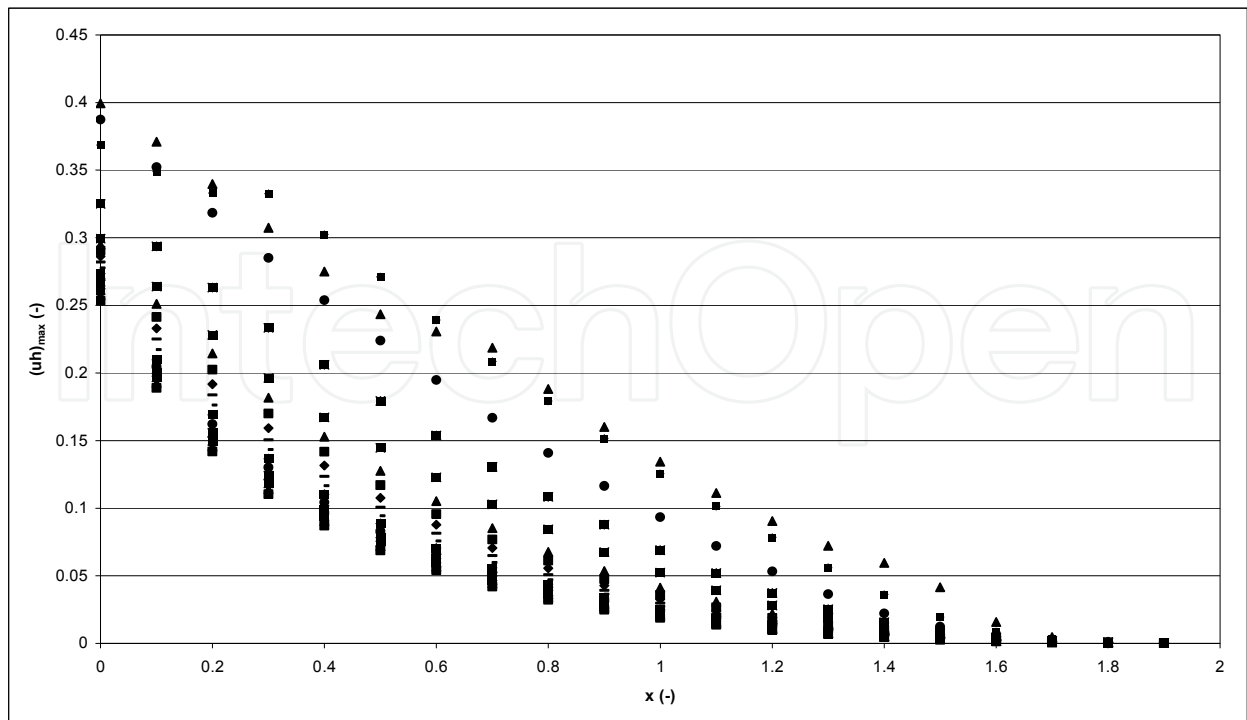
Fig. 13a. Non-dimensional hazard values during uprush versus non-dimensional distance based on Guard and Baldock (2007) solution. Symbols show influence of varying *k*, from *k*=0 to *k*=1.5 at intervals of *k*=0.1.
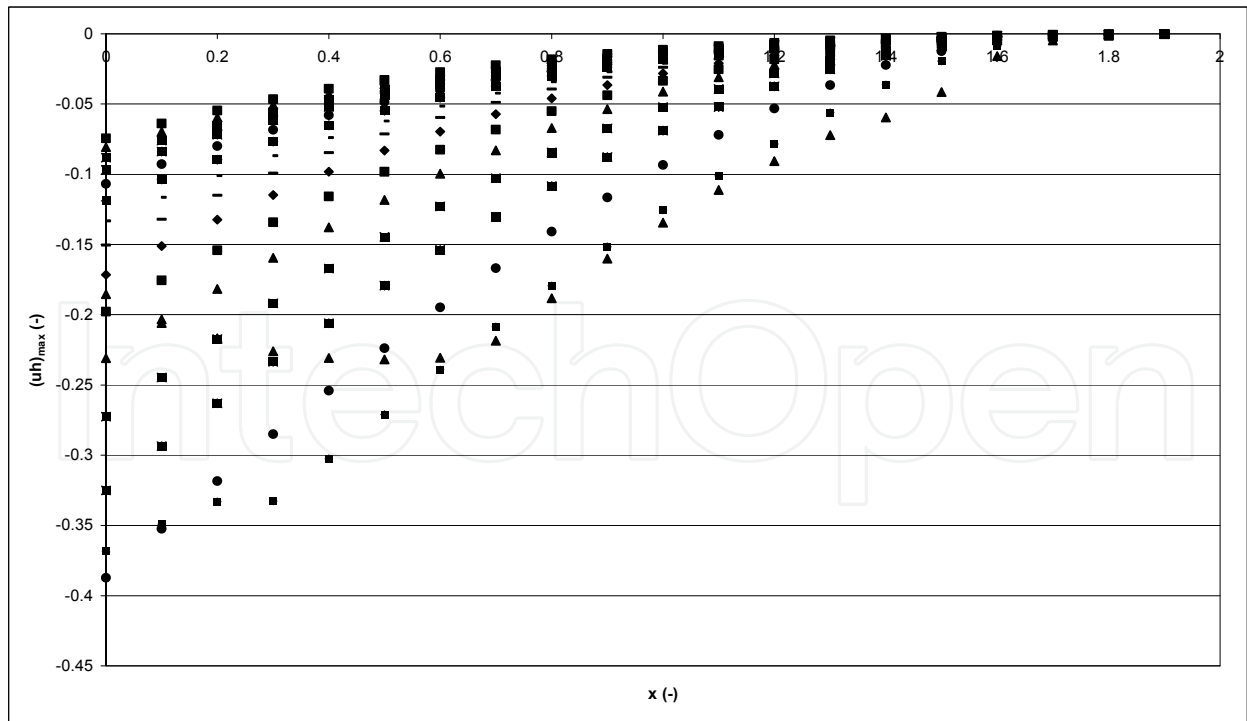

Fig. 13b. Non-dimensional hazard values during backwash versus non-dimensional distance based on Guard and Baldock (2007) solution. Symbols show influence of varying *k*, from *k*=0 to *k*=1.5 at intervals of *k*=0.1.

The hazard during uprush and backwash is approximately equal, although the resulting danger from being carried seaward is probably greater than that of being carried landward. The influence of the boundary conditions and inflow is again very important, and the Shen and Meyer solution is clearly not conservative. Variations in k lead to changes in the values of uh and u^*h^* of a factor 2-6, with greatest variation in the mid-part of the run-up zone.

5.2 Fluid forces

A similar analysis can be performed for the fluid forces, which for surface piercing structures are proportional to the momentum flux, u^2h, as given in (9), and assuming a constant drag coefficient. The maximum flow velocity within the swash zone does not vary as much as the depth varies as the parameter k is changed for different inflow conditions. This is because the maximum velocities are governed by the speed of the advancing and receding shoreline, and the Guard and Baldock solutions converge asymptotically to the Shen and Meyer solution close to the shoreline. Hence, the variation in the forces during uprush and backwash are not as great as those for the water depth (figures 14a&b). Nevertheless, variations in k still lead to variations in the likely fluid forces of a factor 2 in the uprush and a factor 4 in the backwash. Forces in the backwash are a little higher than in the uprush. The key point, however, is that the Shen and Meyer solution is not conservative and predicts the minimum hazard that can be expected during bore run-up, as opposed to the maximum hazard, which is likely to be much better described by solutions with $1<k<1.5$. Yeh (2006) provided a similar analysis for the Shen and Meyer (1963) swash solution (i.e. equivalent to $k=0$). Here, figures 14a&b, in conjunction with (9), enable the values of $u^2{}^*h^*$ to be determined for any location in the run-up zone for any particular bore run-up amplitude and different values for k.
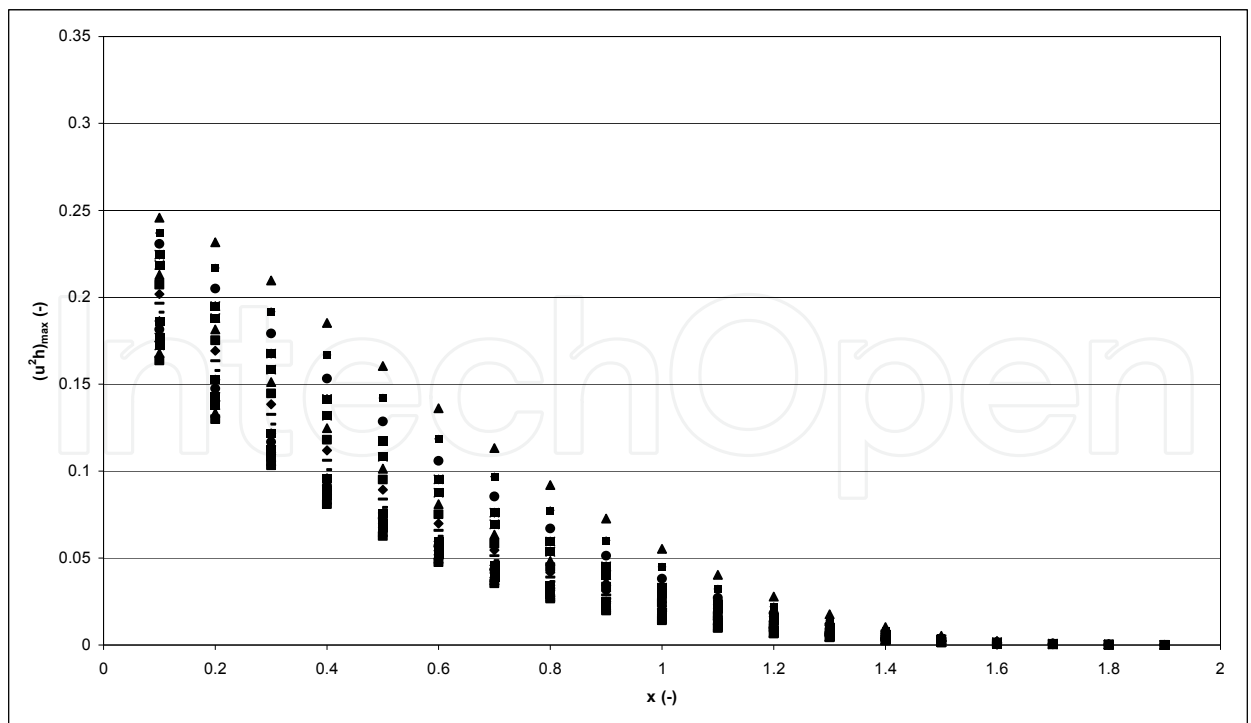

Fig. 14a. Non-dimensional force during uprush versus non-dimensional distance based on Guard and Baldock (2007) solution. Symbols show influence of varying k, from $k=0$ to $k=1.5$ at intervals of $k=0.1$.
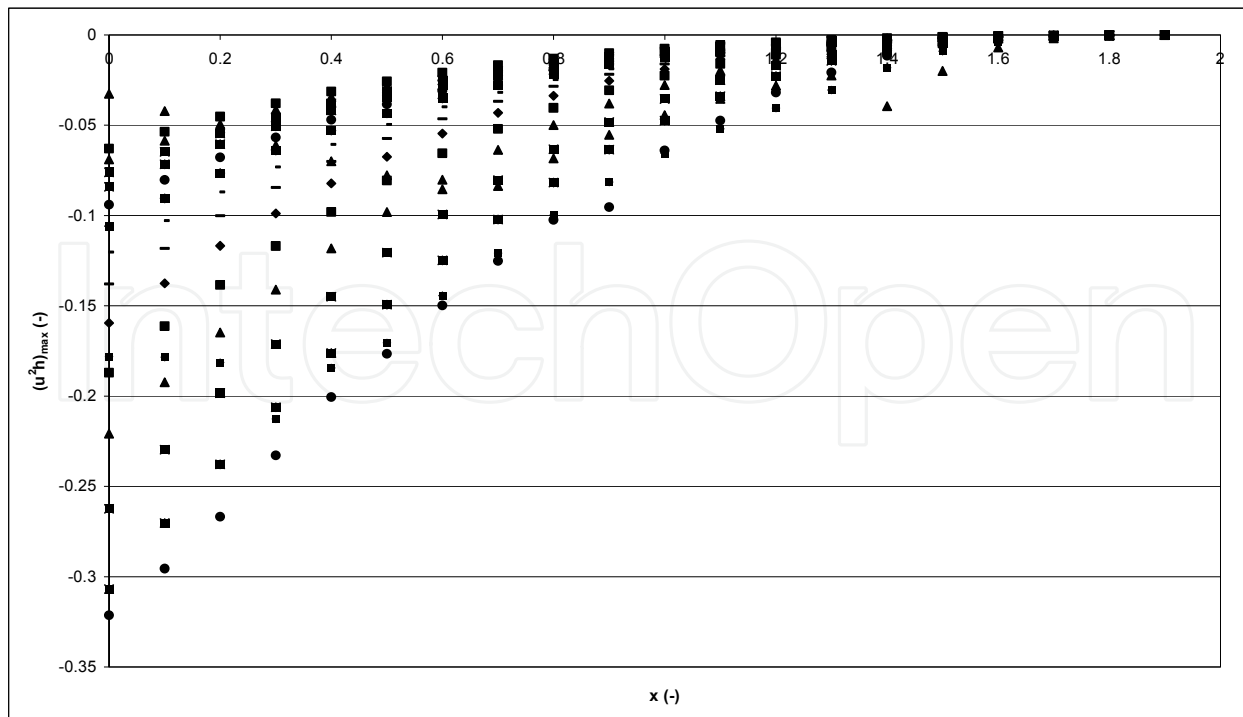
Fig. 14b. Non-dimensional force during backwash versus non-dimensional distance based on Guard and Baldock (2007) solution. Symbols show influence of varying *k*, from *k*=0 to *k*=1.5 at intervals of *k*=0.1.

6. Conclusion

New experimental data on the run-up and overtopping of solitary waves and solitary bores has been presented. The data are discussed with regard to the classical solutions to the non-linear shallow water wave equations and more recent theory. The results show that the Shen and Meyer (1963) swash solution is not conservative in terms of predicting overtopping or overwash flow volumes on beaches and mildly sloping structures. The actual overtopping volumes may be an order of magnitude greater. Further, that solution underestimates hazards in the run-up zone. More recent solutions (Guard and Baldock, 2007) show good agreement with the overtopping data, and demonstrate the difference in flow conditions that arises from different conditions at the seaward swash boundary. This may explain the considerable degree in the variation of overtopping rates in other data sets, previously attributed to scatter. Hence, a range of severity of the hazard can be expected, depending on the wave form. The results are discussed in terms of their applicability to tsunami modelling and evacuation and emergency management strategies.

7. References

Abt, S.R., Wittler, R.J., Taylor, A. and Love, D.J., 1989. Human stability in a high flood zone. *Water Resources Bulletin*, 25(4): 881-890.

Baldock, T.E., 2006. Long wave generation by the shoaling and breaking of transient wave groups on a beach. *Proceedings of the Royal Society A-Mathematical Physical and Engineering Sciences*, 462(2070): 1853-1876.

Baldock, T.E., Cox, D., Maddux, T., Killian, J. and Fayler, L., 2009. Kinematics of breaking tsunami wavefronts: A data set from large scale laboratory experiments. *Coastal Engineering*, 56(5-6): 506-516.

Baldock, T.E., Hughes, M.G., Day, K. and Louys, J., 2005. Swash overtopping and sediment overwash on a truncated beach. *Coastal Engineering*, 52(7): 633-645.

Barnes, M.P. and Baldock, T.E., 2010. A lagrangian model for boundary layer growth and bed shear stress in the swash zone. *Coastal Engineering*, 57(4): 385-396.

Carrier, G.F., Wu, T.T. and Yeh, H., 2003. Tsunami run-up and draw-down on a plane beach. *J. Fluid Mech.*, 475: 79-99.

Dodd, N., 1998. Numerical model of wave run-up, overtopping, and regeneration. *Journal of Waterway Port Coastal and Ocean Engineering-Asce*, 124(2): 73-81.

Donnelly, C., Kraus, N. and Larson, M., 2006. State of knowledge on measurement and modeling of coastal overwash. *Journal of Coastal Research*, 22(4): 965-991.

Goda, Y., 2009. Derivation of unified wave overtopping formulas for seawalls with smooth, impermeable surfaces based on selected clash datasets. *Coastal Engineering*, 56(4): 385-399.

Goring, D.G., 1979. Tsunamis - the propagation of long waves on to a shelf, California Institute of Technology, Pasadena, 337 pp.

Guard, P.A. and Baldock, T.E., 2007. The influence of seaward boundary conditions on swash zone hydrodynamics. *Coastal Engineering*, 54(4): 321-331.

Guard, P.A., Baldock, T.E. and Nielsen, P., 2005. General solutions for the initial run-up of a breaking tsunami front, International Symposium on Disaster Reduction on Coasts, Melbourne.

Hall, J.V. and Watts, J.W., 1953. Laboratory investigation of the vertical rise of solitary waves on impermeable slopes. , Tech. Memo. 33, Beach Erosion Board, USACE.

Hibberd, S. and Peregrine, D.H., 1979. Surf and run-up on a beach: A uniform bore. *J. Fluid Mech.*, 95(2): 323-345.

Hogg, A.J., Baldock., T.E. and Pritchard, D., 2010. Overtopping a truncated planar beach. Journal of Fluid Mechanics, in press.

Hughes, S.A. and Nadal, N.C., 2009. Laboratory study of combined wave overtopping and storm surge overflow of a levee. *Coastal Engineering*, 56: 244-259.

Ingram, D.M., Gao, F., Causon, D.M., Mingham, C.G. and Troch, P., 2009. Numerical investigations of wave overtopping at coastal structures. *Coastal Engineering*, 56(2): 190-202.

Kobayashi, N. and Wurjanto, A., 1989. Wave overtopping on coastal structures. *Journal of Waterway Port Coastal and Ocean Engineering-Asce*, 115(2): 235-251.

Kraus, N.C., Militello, A. and Todoroff, G., 2002. Barrier breaching processes and barrier spit breach, stone lagoon, california. *Shore and Beach*, 70: 21-28.

Madsen, P.A., Fuhrman, D.R. and Schaeffer, H.A., 2008. On the solitary wave paradigm for tsunamis. *Journal of Geophysical Research-Oceans*, 113(C12).

Nielsen, P. and Baldock, T.E., 2010. I-shaped surf beat understood in terms of transient forced long waves. *Coastal Engineering*, 57(1): 71-73.

Peregrine D.H., 1967. Long waves on a beach. *Journal of Fluid Mechanics*, 27: 815-830.

Peregrine and H., D., 1966. Calculations of development of an undular bore. *Journal of Fluid Mechanics*, 25: 321-330.

Peregrine, D.H. and Williams, S.M., 2001. Swash overtopping a truncated plane beach. *J. Fluid Mech.*, 440: 391-399.

Power, H.E., Palmsten, M., Holman, R.A. and Baldock, T.E., 2009. Remote sensing of swash zone boundary conditions using video and argus, Coastal Dynamics 2009. ASCE, Tokyo.

Pritchard, D., Guard, P.A. and Baldock, T.E., 2008. An analytical model for bore-driven runup. *Journal of Fluid Mechanics*, 610(1): 193.

Pritchard, D. and Hogg, A.J., 2005. On the transport of suspended sediment by a swash event on a plane beach. *Coastal Engineering*, 52(1): 1-23.

Ramsbottom, D., P. Floyd and Penning-Rowsell., E., 2003. Flood risks to people phase 1, r&d technical report, fd2317defra DEFRA / Environment Agency, Flood Management Division, London, UK, London.

Shen, M.C. and Meyer, R.E., 1963. Climb of a bore on a beach. Part 3. Runup. *J. Fluid Mech.*, 16: 113-125.

Stansby, P.K., 2003. Solitary wave run up and overtopping by a semi-implicit finite-volume shallow-water boussinesq model. *Journal of Hydraulic Research*, 41(6): 639-647.

Synolakis, C.E., 1987. The runup of solitary waves. *J. Fluid Mech.*, 185: 523-545.

Synolakis, C.E. and Bernard, E.N., 2006. Tsunami science before and beyond boxing day 2004. *Philosophical Transactions of the Royal Society A-Mathematical Physical and Engineering Sciences*, 364(1845): 2231-2265.

Yeh, H., 2006. Maximum fluid forces in the tsunami runup zone. *Journal of Waterway Port Coastal and Ocean Engineering-Asce*, 132(6): 496-500.

Yeh, H.H., 1991. Tsunami bore runup. *Natural Hazards*, 4: 209–220.

The Tsunami Threat - Research and Technology
Edited by Nils-Axel Mörner

Submarine earthquakes, submarine slides and impacts may set large water volumes in motion characterized by very long wavelengths and a very high speed of lateral displacement, when reaching shallower water the wave breaks in over land - often with disastrous effects. This natural phenomenon is known as a tsunami event. By December 26, 2004, an event in the Indian Ocean, this word suddenly became known to the public. The effects were indeed disastrous and 227,898 people were killed. Tsunami events are a natural part of the Earth's geophysical system. There have been numerous events in the past and they will continue to be a threat to humanity; even more so today, when the coastal zone is occupied by so much more human activity and many more people. Therefore, tsunamis pose a very serious threat to humanity. The only way for us to face this threat is by increased knowledge so that we can meet future events by efficient warning systems and aid organizations. This book offers extensive and new information on tsunamis; their origin, history, effects, monitoring, hazards assessment and proposed handling with respect to precaution. Only through knowledge do we know how to behave in a wise manner. This book should be a well of tsunami knowledge for a long time, we hope.

How to reference
In order to correctly reference this scholarly work, feel free to copy and paste the following:

Tom E. Baldock and Damitha Peiris (2011). Overtopping and Run-up Hazards Induced by Solitary Waves and Bores, The Tsunami Threat - Research and Technology, Nils-Axel Mörner (Ed.), ISBN: 978-953-307-552-5, InTech, Available from: http://www.intechopen.com/books/the-tsunami-threat-research-and-technology/overtopping-and-run-up-hazards-induced-by-solitary-waves-and-bores

INTECH
open science | open minds